ACS SyntheticBiology

Research Article

pubs.acs.org/synthbio

Computer-Assisted Engineering of the Synthetic Pathway for Biodegradation of a Toxic Persistent Pollutant

Nagendra Prasad Kurumbang,[†,⊥] Pavel Dvorak,[†,‡,⊥] Jaroslav Bendl,[†,§] Jan Brezovsky,[†] Zbynek Prokop,*[,†,‡] and Jiri Damborsky*[,†,‡]

[†]Loschmidt Laboratories, Department of Experimental Biology and Research Centre for Toxic Compounds in the Environment, Faculty of Science, Masaryk University, Kamenice 5/A13, 625 00 Brno, Czech Republic

[‡]International Clinical Research Center, St. Anne's University Hospital Brno, Pekarska 53, 656 91 Brno, Czech Republic

[§]Department of Information Systems, Faculty of Information Technology, Brno University of Technology, Bozetechova 1, 612 00 Brno, Czech Republic

Supporting Information

ABSTRACT: Anthropogenic halogenated compounds were unknown to nature until the industrial revolution, and microorganisms have not had sufficient time to evolve enzymes for their degradation. The lack of efficient enzymes and natural pathways can be addressed through a combination of protein and metabolic engineering. We have assembled a synthetic route for conversion of the highly toxic and recalcitrant 1,2,3-trichloropropane to glycerol in *Escherichia coli*, and used it for a systematic study of pathway bottlenecks. Optimal ratios of enzymes for the maximal production of glycerol, and minimal toxicity of metabolites were predicted using a mathematical model. The strains containing the expected optimal ratios of enzymes were constructed and characterized for their viability and degradation efficiency. Excellent agreement between predicted and experimental data was observed. The validated model was used to quantitatively describe the kinetic limitations of currently available enzyme variants and predict improvements required for further pathway optimization. This highlights the potential of forward engineering of microorganisms for the degradation of toxic anthropogenic compounds.

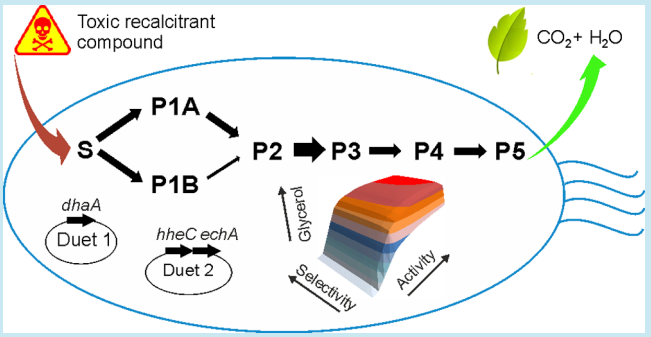

KEYWORDS: *activity, enantioselectivity, kinetic modeling, protein and metabolic engineering, synthetic pathway, toxicity*

Halogenated hydrocarbons, which are often anthropogenic compounds, are widely used for agricultural, industrial and military purposes.[1] Once introduced into the environment, these halogenated hydrocarbons often persist and cause a serious threat to natural ecosystems and human health. Natural catabolic pathways for their mineralization are inefficient or lacking, primarily due to the fact that most of the discussed chemicals were present in the environment until last century. Engineering bacteria toward enhanced biodegradation capacities has been intensively studied; however, only limited success has been achieved so far.[2,3] One of the most common failures is because of an imbalance in the expression or catalytic properties of enzymes employed in synthetic routes. This factor often leads to an accumulation of toxic intermediates, insufficient flux through the pathway, and limited fitness of the host organism.[4−8]

A number of approaches dealing with the unbalanced properties of enzymes in engineered pathways have been reported in recent years. Improvement of pathway performance can be achieved through the introduction of engineered enzyme variants,[9,10] kinetic modeling of the system[11,12] or modular optimization of the pathway.[13−15] Although these examples come predominantly from the field of biosynthesis of valuable chemicals, adoption of such synthetic biology tools holds considerable promise for rational tuning of pathways for biodegradation of industrial waste.[16]

1,2,3-Trichloropropane (TCP) is a man-made compound, produced as a byproduct during the commercial manufacture of epichlorohydrin, and used as an intermediate in chemical industries and as a solvent for oils, fats, waxes, and resins.[17] It is an emerging toxic groundwater pollutant and suspected carcinogen, which spreads to the environment mainly due to improper waste management.[17−19] No naturally occurring bacterial strain capable of aerobic utilization of TCP has been isolated from nature thus far. However, TCP can be converted to harmless glycerol (GLY) via a five-step catabolic pathway assembled with haloalkane dehalogenase (DhaA)[20] from *Rhodococcus rhodochrous* NCIMB 13064, haloalcohol dehalogenase (HheC),[21] and epoxide hydrolase (EchA)[22] from *Agrobacterium radiobacter* AD1 (Figure 1). The first recombinant strain partially degrading TCP was constructed using heterolo-

Special Issue: SB6.0

Received: September 26, 2013

dx.doi.org/10.1021/sb400147n | *ACS Synth. Biol.* XXXX, XXX, XXX−XXX

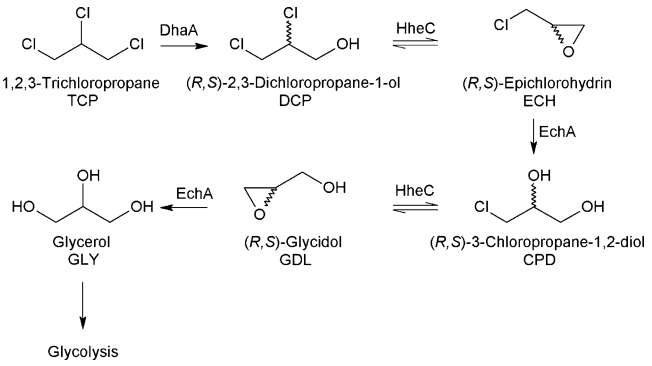

Figure 1. A synthetic pathway for the biodegradation of TCP assembled in *Escherichia coli* BL21 (DE3). Enzyme sources: DhaA[20] from *Rhodococcus rhodochrous* NCIMB 13064, HheC[21] from *Agrobacterium radiobacter* AD1, and EchA[22] from *Agrobacterium radiobacter* AD1.

gous expression of DhaA or an 8-times more active mutant form of DhaAM2 in its natural host *A. radiobacter* AD1, possessing the remainder of the pathway.[23,24] Although some increase in optical density of cultures were observed in the latter case, the efficiency of TCP mineralization was insufficient for supporting significant growth. It was proposed that the poor activity of haloalkane dehalogenase toward TCP, and formation of toxic intermediates represent primary bottlenecks of the pathway. Furthermore, equimolar production of the (*S*) and (*R*) enantiomers of 2,3-dichloropropane-1-ol (DCP) from prochiral TCP by non-selective DhaA and the resulting accumulation of (*S*)-DCP caused by high enantioselectivity of HheC toward (*R*)-DCP was observed and discussed as the factor limiting the flux of carbon through the pathway. The effects of the described bottlenecks in the context of the whole synthetic pathway have not been studied in detail.

Significant efforts have been invested in the past few years in engineering the first enzyme of the TCP pathway: haloalkane dehalogenase (DhaA).[25−28] Constructed mutants can possibly help overcome the previously mentioned limitations of the TCP pathway. Mutant DhaA31, constructed in our laboratory using computer-assisted directed evolution, showed 26-fold higher catalytic efficiency toward TCP than the wild type enzyme (DhaAwt: k_{cat} = 0.04 s^{-1}, k_{cat}/K_m = 40 s^{-1} M^{-1}; DhaA31: k_{cat} = 1.26 s^{-1}, k_{cat}/K_m = 1050 s^{-1} M^{-1}), while its enatioselectivity with the same substrate remained unchanged.[26] Mutant r5−90R (referred here as DhaA90R), obtained after five rounds of directed evolution of DhaA31 by van Leeuwen et al.,[27] converted prochiral TCP predominantly into (*R*)-DCP (ee 90%), which is the preferred substrate for the selective HheC. DhaA90R possessed similar catalytic efficiency toward TCP as the wild-type enzyme (k_{cat} = 0.16 s^{-1}; k_{cat}/K_m = 25 M^{-1} s^{-1}). Thus each of the mutants, DhaA31 and DhaA90R, show improvement in one of the limiting factors of the TCP pathway.

In this study, we carried out a systematic analysis and rational optimization of the synthetic metabolic pathway for the biodegradation of TCP. Both engineered variants of DhaA were integrated to evaluate the effects of increased activity and improved selectivity on the performance of the pathway. A recently developed kinetic model[29] with newly incorporated toxicity and plasmid parameters was employed for rational selection of suitable plasmid combinations and balancing the stoichiometry of the enzyme DhaA/DhaA31/DhaA90R:HheC:EchA. The pathway was optimized toward faster removal of toxic metabolites and higher production of GLY. Several *E. coli* constructs were prepared on the basis of the predictions and characterized for their viability and ability to degrade TCP. Advantages and limitations of the engineered DhaA variants in the context of the pathway were analyzed, and obtained information was used to propose further optimization steps.

RESULTS AND DISCUSSION

The haloalkane dehalogenase DhaA, the haloalcohol dehalogenase HheC, and the epoxide hydrolase EchA were transferred into a heterologous host, *Escherichia coli* BL21 (DE3), for systematic analysis and rational optimization of a synthetic metabolic pathway for the biodegradation of TCP. The three enzymes and five metabolites of the pathway do not naturally occur in *E. coli*, making this system suitable for the analysis of pathway bottlenecks.

Toxicity of TCP and Intermediate Metabolites for *E. coli*. Both toxicity of metabolites and the flux of carbon through the pathway represent the factors dictating the viability of the host organism. Toxicity of TCP and its metabolites toward *E. coli* has not been reported. Thus, we tested the effects of various concentrations of TCP, DCP, epichlorohydrin (ECH), 3-chloropropane-1,2-diol (CPD) and glycidol (GDL) on growth of the *E. coli* BL21 (DE3) culture in mineral medium supplied with glucose. The concentration at which 20% of the total cell population was inhibited (IC_{20}) was calculated for each compound (Figure S1, Supporting Information). Results revealed that TCP and epoxide ECH are the most toxic among all the tested compounds with IC_{20} values of 1.35 and 1.41 mM, respectively (Figure 2). The toxicity of both halogenated

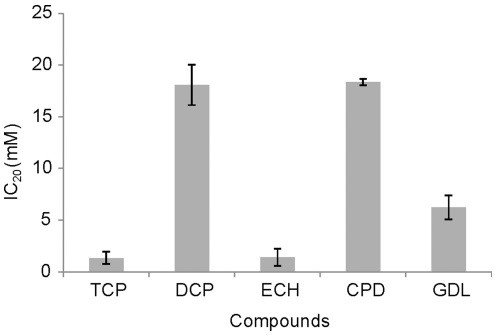

Figure 2. Toxicity of TCP and intermediate metabolites for *E. coli* BL21 (DE3). Toxicity is expressed as inhibition concentration IC_{20}.

alcohols, out of which DCP tends to accumulate in the pathway, was 1 order of magnitude lower. The second epoxide, GDL, had an intermediate toxic effect with an IC_{20} of 6.25 mM. The analysis of TCP, DCP, and GDL accumulation in *E. coli* showed that TCP is the only compound that has the potential for cellular accumulation due to its higher hydrophobicity (Table S1, Supporting Information). The hydrophobicity and accumulation of the other metabolites was significantly lower because of the introduced polar hydroxyl groups. These results suggest that concentrations of metabolites from the TCP pathway detected in the supernatant of the buffer or medium are a good representation of their intracellular concentrations.

Construction of TCP Degraders by the Assembly of an Engineered Pathway in *E. coli*. The TCP pathway was assembled in two modules, separating expression of the first enzyme (DhaA) from expression of the second and third enzymes (HheC and EchA). The two major bottlenecks of the pathway, (i) poor activity of the first enzyme with TCP and (ii)

dx.doi.org/10.1021/sb400147n | *ACS Synth. Biol.* XXXX, XXX, XXX−XXX

Table 1. Theoretical and Experimental (in Bold) Ratios of Enzymes in the Constructed Degraders

degrader	plasmid combinations	theoretical and experimental ratio DhaA:HheC:EchA	sum of enzymes[a]
degWT	pCDF-dhaAwt + pETDuet-echA-hheC	0.20:0.40:0.40	
		0.28:0.38:0.34	1.00
degWT-opt	pETDuet-dhaAwt + pCDF-echA-hheC	0.50:0.25:0.25	
		0.56:0.25:0.19	0.94
deg90R	pCDF-dhaA90R + pETDuet-echA-hheC	0.20:0.40:0.40	
		0.16:0.40:0.45	1.03
deg90R-opt	pETDuet-dhaA90R + pACYC-echA-hheC	0.67:0.16:0.17	
		0.70:0.12:0.18	0.95
deg31	pCDF-dhaA31 + pETDuet-echA-hheC	0.20:0.40:0.40	
		0.12:0.42:0.46	1.06
deg31-opt	pCDF-dhaA31 + pACYC-echA-hheC	0.50:0.25:0.25	
		0.60:0.16:0.24	0.74

[a]The sum of the three enzymes in each degrader was calculated from the density of corresponding bands on SDS-PAGE gels and compared to the degWT value (set as 1.00).

formation of toxic intermediates, were thus dissected. Modular assembly of the pathway was carried out using combinations of two out of three Duet vectors: pACYCDuet-1, pCDFDuet-1, and pETDuet-1.[30] The Duet vector system has already proven its utility in modular engineering of biosynthetic multienzyme pathways.[15,31−33] Individual Duet vectors can be combined in a single host cell due to the different origins of the replication and antibiotic resistance marker (see Table 2).[34] The modular expression strength can be calculated using the promoter strength and plasmid copy number.[13,15,33,34] The expression levels of subcloned genes can be estimated from the copy numbers of combined plasmids, since all Duet vectors contain the same *T7* promoter and the differences in expression of individual genes from the TCP pathway under this promoter were found to be negligible (Figure S2, Supporting Information).

The starting variants of the TCP pathway were constructed by subcloning *dhaA*wt, *dhaA*90R or *dhaA*31 into the second multiple cloning site of pCDFDuet-1, and *echA* and *hheC* into the first and second multiple cloning sites of pETDuet-1, respectively. This combination should provide an almost equal ratio of subcloned enzymes based on reported copy numbers of used plasmids. The combination of plasmids, consisting of the first enzyme (DhaA) in pCDFDuet-1, and the second and third (HheC and EchA) enzymes in pETDuet-1, was the same in all three variants. Plasmid pairs were cotransformed into *E. coli*, resulting in three constructs denoted degWT, deg90R, and deg31 (Table 1). Degraders were cultivated in LB medium using a standardized cultivation protocol. An approximate estimation of expression profiles obtained from sodium dodecyl sulfate polyacrylamide gel electrophoresis (SDS-PAGE) analysis of cell free extract (CFE) showed that the relative ratio of enzymes in the three degraders was close to 0.2:0.4:0.4 (Figure S3, Supporting Information).

Optimization of the ratio of the three enzymes in the TCP pathway was conducted using an extended version of the previously developed kinetic model.[29] The model is based on the Michaelis−Menten steady-state kinetic parameters of DhaA variants, HheC, and EchA, determined with their corresponding substrates *in vitro*. The concentration of each enzyme is kept constant at 0.1 mg/mL. New constraints defining the toxicity of individual metabolites and copy numbers of the used plasmids determining the expression level of enzymes were introduced for optimization of the pathway *in vivo*. The model was used to calculate all possible combinations of the two plasmids within the defined constraints (Tables S2−S4, Supporting Information). Calculated time courses of the modeled multienzyme conversion of 2 mM TCP at a time interval of 300 min were visualized using Gnuplot (Figures S4−S6, Supporting Information). Twelve resulting combinations for each of the pathway variants and the corresponding twelve relative expression ratios were ranked according to (i) the efficiency of GLY production and (ii) the level of the overall toxicity in the system, assuming additivity of the metabolites' toxic effects. Plasmid combinations used in the nonoptimized degraders degWT, deg90R, and deg31 (pCDF-dhaA variant+pETDuet-echA-hheC) were ranked lower compared to highly ranked degraders with optimized expression levels.

A single combination of plasmids (pETDuet-dhaA90R +pACYC-echA-hheC) showed the best rank, leading to the highest GLY production and the lowest toxicity for the degrader employing the DhaA90R variant (Table S3, Supporting Information). Variants with DhaAwt and DhaA31 showed three and four equally good combinations, respectively, from which one combination was selected for experimental construction (Tables S2 and S4, Supporting Information). The plasmid combination pETDuet-dhaAwt+pCDF-echA-hheC was selected for degWT-opt and pCDF-dhaA31+pACYC-echA-hheC for deg31-opt (Table 1). Comparison of the calculated values representing GLY production and overall toxicity showed that both degWT-opt and deg90R-opt produced 2-fold more GLY and less toxic metabolites, in comparison to degWT and deg90R (Tables S2 and S3, Supporting Information). Calculated values for plasmid combinations bearing genes of catalytically efficient DhaA31 plus HheC and EchA showed that this biochemical pathway cannot be effectively optimized for GLY production within the defined constraints (Table S4, Supporting Information), and deg31-opt was expected to provide improvement only in terms of a lower level of toxic metabolites.

Experimental Characterization of the TCP Degraders. The resting cells of six degraders were experimentally characterized in terms of their (i) expression profile, (ii) viability, and (iii) degradation capacity. The degraders were cultivated in LB medium using a standardized cultivation protocol with heterologous protein expression induced by isopropyl-β-D-thiogalactopyranoside (IPTG). The degraders with overexpressed enzymes of the TCP pathway were harvested and disintegrated using sonication. Equal amounts of CFEs were loaded on SDS-PAGE, and the expression profiles of six degraders were analyzed by densitometry (Figure 3). Relative ratios of DhaA variants, HheC and EchA were calculated from

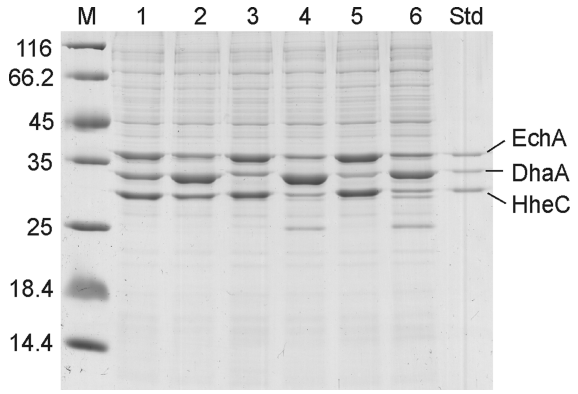

Figure 3. SDS-PAGE analysis of the expression profiles of the six constructed degraders. M: protein marker (units in kDa), 1: degWT, 2: degWT-opt, 3: deg90R, 4: deg90R-opt, 5: deg31, 6: deg31-opt, and Std: standard sample with purified DhaAwt, HheC, and EchA containing 0.25 μg of each enzyme. The theoretical molecular weights of the DhaA variants, HheC and Echa are 34, 29, and 35 kDa, respectively.

band densities and compared with the theoretical relative ratios predicted by modeling (Table 1). An excellent agreement between theoretical and experimental values was observed. The relative sum of the three enzymes from the TCP pathway was calculated as a sum of the band densities and revealed that degraders with an optimized ratio contained equal or lower total amounts of the enzymes than nonoptimized ones.

The viability and ability to degrade TCP was tested with resting cells of the degraders resuspended in synthetic mineral medium (SMM) with a final OD_{600} of 0.1. Cells were incubated at 30 °C with 2 mM TCP and no additional carbon source. Time course of TCP and DCP concentrations was monitored by GC analysis over 120 h (Figure 4A–C). No significant accumulation of other metabolites of the TCP pathway was observed. Viabilities of the six degraders and host with and without TCP as controls are presented in Figure 4D. No GLY was detected in cell cultures suggesting its utilization by the cells. The production of GLY via the TCP pathway was confirmed in parallel by incubation of induced cells of deg31 and deg31-opt in the presence of 2 mM TCP and 5 mM glucose (Figure S7,

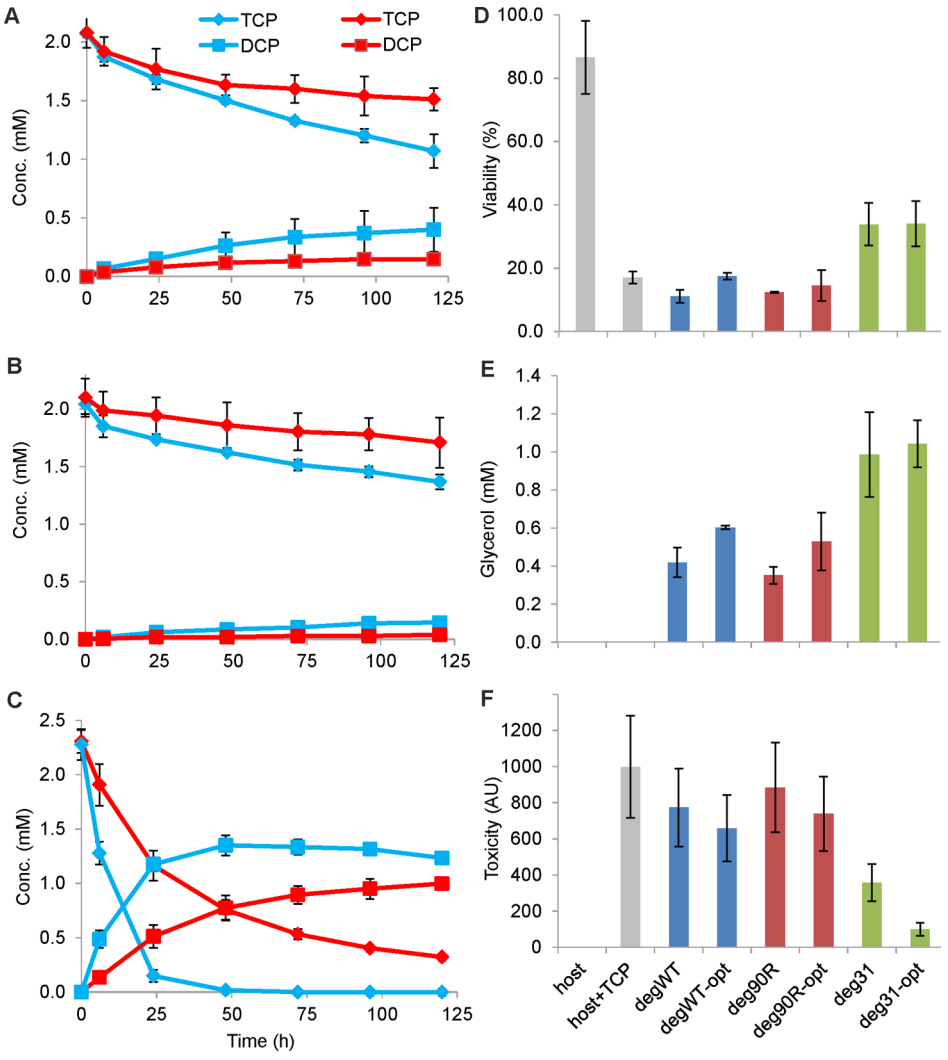

Figure 4. Degradation profiles and viability of the six degraders. (A–C) Degradation profiles of the degraders containing DhaAwt, DhaA90R, and DhaA31, respectively. The diamonds and squares refer to concentrations of TCP and DCP of nonoptimized (red) and optimized (blue) variants. (D) Viability of the host and degraders after 120 h incubation in SMM medium with TCP, relative to the viability at the beginning of the experiment. (E) GLY production calculated from concentrations of TCP and DCP detected at the end of incubation. (F) Overall toxicity of metabolites to degraders presented in arbitrary units (AU). Standard deviations were obtained from three independent experiments.

dx.doi.org/10.1021/sb400147n | *ACS Synth. Biol.* XXXX, XXX, XXX–XXX

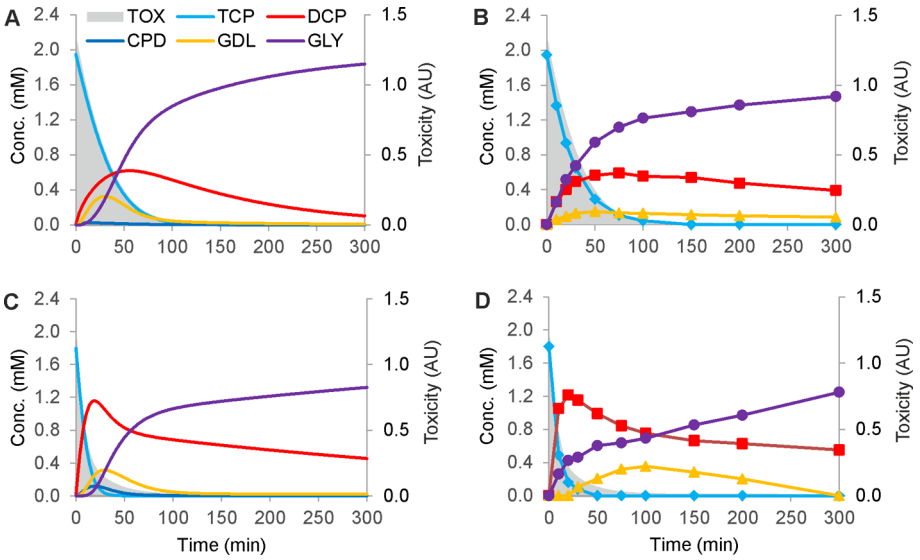

Figure 5. Predicted and experimentally determined degradation profiles of constructs containing the engineered haloalkane dehalogenase DhaA31. Theoretical (A) and experimental (B) profiles of deg31; theoretical (C) and experimental (D) profiles of deg31-opt. Toxicity is denoted as the gray area under the graph and given in arbitrary units (AU). Concentrations of GLY were calculated from concentrations of other detected metabolites. Experimental data points are the mean values of two replicates.

Supporting Information). Theoretical concentrations of produced GLY in cultures without glucose and relative toxicity for each degrader were calculated from recorded time course concentrations of TCP and DCP (Figure 4E,F).

The averaged data from the three independent experiments revealed that all three degraders with rationally optimized ratios of pathway enzymes degraded TCP faster than nonoptimized constructs. Experimental time courses of TCP and DCP concentrations correlated with the relative ratios of enzymes in the degraders. Differences in profiles corresponded to the catalytic parameters of the DhaA variant and the relative ratio of haloalkane dehalogenase with respect to the other two associated enzymes (Figure 4A–C and Table 1). Deg90R and deg90R-opt with selective DhaA90R showed minimal accumulation of DCP, but their degradation potential was limited by a low catalytic efficiency with TCP. Deg31 and deg31-opt, both containing DhaA31, the nonselective variant with improved catalytic efficiency toward TCP, showed the fastest conversion of TCP, but also the most significant accumulation of DCP. These two effects were even more pronounced in the deg31-opt with higher expression of DhaA31.

Viability reflects the physiological state of the cells heterologously expressing the synthetic pathway after their exposure to toxic TCP (Figure 4D). DegWT-opt showed a small but statistically significant difference in cell viability compared to degWT, suggesting that optimization of the expression levels provided benefits to the cells. The difference in viability of deg90R and deg90R-opt was statistically insignificant: the low production of GLY was not balanced by a higher selectivity of DhaA90R and reduced accumulation of DCP. The most striking result was the superior viability of both degraders containing the DhaA31 enzyme, connected to a higher production of GLY and/or reduced toxicity compared to the degraders expressing DhaAwt and DhaA90R. Deg31-opt removes the toxic metabolites faster than deg31, but the effect of the reduced toxicity on the viability of this degrader is not visible, suggesting that both degraders surpassed some threshold level beyond which toxicity does not play a role and only the amount of produced GLY is the key factor determining cell viability. Further improvement in viability should be achieved by a more efficient production of GLY. Approximately 1 mM concentration of GLY produced within 5 days by the best variants, deg31 and deg31-opt, is probably not sufficient to provide energy for growth and compensation for the oxidative stress induced during the aerobic mineralization of toxic chlorinated substrates.[35]

The ability of the degraders to recover from short-term (300 min) exposure to a higher concentration (3.5 mM) of TCP was tested (Figure S8, Supporting Information). Resulting growth curves corresponded well with the viabilities of degraders calculated from plating after 120 h incubation with a lower concentration of TCP. Only deg31 and deg31-opt recovered faster than the host BL21 (DE3) without the synthetic pathway (control) and with comparable growth. Degraders degWT and deg90R, with a nonoptimized ratio of pathway enzymes, and deg90R-opt, with an optimized ratio but poor conversion of TCP, recovered slower than the control. Only degWT-opt showed comparable growth with host cells without the introduced pathway, again confirming the benefits of pathway optimization. The data confirm that the constructs containing DhaA31 are not significantly affected by an increased metabolic burden.[36]

Identification of Pathway Bottlenecks. Two constructs carrying DhaA31 and showing the highest viability were selected for further characterization. Preinduced cells of elevated cell densities (OD_{600} 3.5) were used to secure complete degradation of 2 mM TCP during a shorter incubation time (300 min). The mass ratio of enzymes in both degraders was estimated by SDS-PAGE and verified with measurements of catalytic activities in CFE (Table S5, Supporting Information). Obtained data were used for determination of the enzyme concentrations and applied to calculations of the degradation profiles of deg31 and deg31-opt. In both cases the experimental profiles showed a good agreement with predictions (Figure 5). Accumulation of DCP and GDL was observed for both constructs. A more pronounced accumulation of DCP was observed for deg31-opt, with faster removal of TCP and a corresponding lower toxicity of the system. The accumulated DCP was analyzed by chiral GC and found to be mainly composed of the (*S*)-enantiomer (Figure S7

dx.doi.org/10.1021/sb400147n | *ACS Synth. Biol.* XXXX, XXX, XXX–XXX

Supplementary Information). Theoretical conversions of TCP to GLY at the end of incubation calculated from experimental concentrations of TCP at time 0 min and concentrations of the accumulated metabolites at 300 min was similar for both deg31 and deg31-opt (75 and 69%). This is in agreement with the data previously collected over 120 h for conversion of 2 mM TCP and suggests that the degraders containing DhaA31 cannot be further optimized for better production of GLY without further engineering of DhaA properties (Table S4, Supporting Information).

Currently available DhaA variants with increased activity[26] and improved enantioselectivity[27] provided only partial improvement of the overall efficiency of TCP degradation, even after optimization in the ratio of enzymes of the synthetic pathway. The level of GLY production required for cellular maintenance and growth of the degrader continued to be limited by insufficient selectivity of the DhaA variant with enhanced activity, and *vice versa* by insufficient activity of the variant with increased enantioselectivity. Following these findings, we applied our mathematical model to estimate the effect of catalytic activity and enantioselectivity on the production of GLY (Figure 6). We

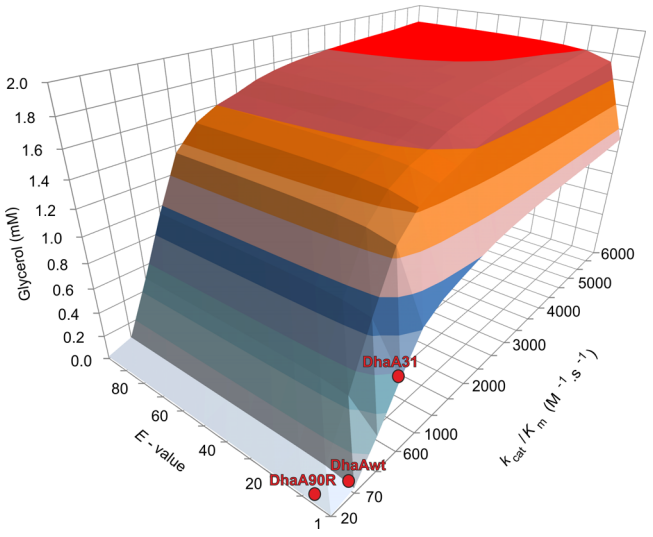

Figure 6. Hypersurface plot describing the effect of catalytic efficiency (k_{cat}/K_m) and enantioselectivity (E-value) of DhaA on the production of GLY. The positions of the three variants of DhaA are indicated by red dots. The substrate TCP is supplied at 2 mM. The kinetic constants of DhaAwt, DhaAR90, and DhaA31 were experimentally determined[29] and differ slightly from data reported in the literature.[26,27]

measured the minimum concentration of GLY required for cellular maintenance and observable growth of the host cells for OD_{600} 0.1 and determined that at least 1 mM of GLY should be supplied to the culture within the time interval of 24 h (Figure S9, Supporting Information). The amount of GLY required for maintenance and growth could be higher in a culture containing toxic substances like TCP and intermediate metabolites due to the extra burden caused by their toxicity. The theoretical production of GLY by the culture of the best degrader deg31-opt with OD_{600} of 0.1 was calculated to be 0.6 mM per 24 h, suggesting that DhaA31 does not possess the required catalytic properties. To increase GLY production to 1 mM per 24 h, the model suggested the need for further improvement of the catalytic efficiency of DhaA31 by 4-fold, or improvement of the enantioselectivity by 20-fold (Figure S10, Supporting Information). Alternatively, the employment of a DhaA variant with combined improvement of catalytic efficiency by 1.2-fold and enantioselectivity by 10-fold in favor of production of (*R*)-DCP would produce 1 mM GLY within 24 h. A DhaA variant possessing the properties enabling the highest possible pathway efficiency (1.6 mM GLY per 24 h) should have 4-fold improvement in catalytic efficiency and 20-fold higher enantioselectivity compared to DhaA31.

Conclusions. The toxicity of the substrate/metabolites and insufficient carbon/energy flow can limit viability of the host organism and represent possible bottlenecks in the TCP degradation pathway. The most toxic substances within the pathway are TCP (IC_{20} = 1.35 mM) and ECH (IC_{20} = 1.41 mM). Other intermediates of the pathway are significantly less toxic. Since accumulation of ECH inside the cells does not take place, the hydrophobic substrate TCP represents the single most important toxic substance of the pathway. A concentration of GLY ≥ 1 mM supports cellular maintenance and growth of *E. coli* BL21 (DE3) with an initial OD_{600} 0.1.

A kinetic model was employed to improve the TCP degradation pathway using engineered enzyme variants and balanced enzyme ratios. Predictions were evaluated in terms of minimized toxicity of intermediates and maximized production of GLY, and showed excellent correspondence with experimental data. Expression levels of the enzymes can also be reliably predicted from a combination of plasmids with different copy numbers. A statistically significant increase in the viability of degWT-opt compared to degWT demonstrates that optimization of the enzyme ratio is a useful approach for improvement of overall pathway performance, and that the kinetic model employing *in vitro* measured kinetic parameters of individual enzymes is applicable for rational pathway engineering. The model can be used for the design of constructs with optimized expression levels and prediction of minimum requirements for catalyst properties.

Toxicity of the substrate does not limit viability of the cells employing the highly active variant of the first enzyme, haloalkane dehalogenase DhaA31, in the pathway. This is due to rapid conversion of the highly toxic TCP to the less toxic DCP. However, the growth and viability of the cells are limited by the insufficient production of GLY. Production of GLY can be improved by further engineering the first enzyme of the pathway toward a higher catalytic efficiency (k_{cat}/K_m > 2300 s^{-1} M^{-1}) or higher enantioselectivy (E-value > 20), or by a combination of both properties (k_{cat}/K_m > 700 s^{-1} M^{-1} and E-value > 10). Removal of the enantioselectivity of the second enzyme in the pathway, haloalcohol dehalogenase HheC, represents another option for improvement of the carbon/energy flow. Construction of a new generation of catalysts for degradation of TCP is currently ongoing in our laboratory.

METHODS

Chemicals, Media, Strains and Plasmids. TCP, DCP, ECH, CPD, GDL and GLY standards were purchased from Sigma-Aldrich (USA). All chemicals used in this study were of analytical grade. All restriction enzymes and DNA ligase were purchased from New England Biolabs (USA). A free Glycerol Assay Kit was acquired from BioVision (USA). Luria Broth (LB) (Sigma Aldrich, USA) was used for routine cultures. A synthetic mineral medium (SMM)[37] containing 5.4 g of $Na_2HPO_4 \cdot 12H_2O$, 1.4 g of KH_2PO_4, 0.5 g of $(NH_4)_2SO_4$, 0.2 g of $MgSO_4 \cdot 7H_2O$, 2 mL of trace elements solution,[38] and 1 mL of vitamin B1 (10 g/mL) per 1 L was used for selection experiments. M9 minimal medium (Sigma Aldrich, USA) containing 0.2 g of

dx.doi.org/10.1021/sb400147n | *ACS Synth. Biol.* XXXX, XXX, XXX−XXX

Table 2. Plasmids Used and Recombinants Constructed

duet vectors[a]	origin	copy no.	cloned gene	recombinant plasmids	restriction sites
pACYCDuet-1[b]	P15A	10−12	*echA, hheC*	pACYC-*echA-hheC*	*echA* (*Nco*I/*Hind*III), *hheC* (*Nde*I/*Kpn*I)
pCDFDuet-1[c]	CloDF13	20−40	*dhaAwt*	pCDF-*dhaA*wt	*Nde*I/*Kpn*I
			dhaA31	pCDF-*dhaA*31	*Nde*I/*Xho*I
			dhaA90R	pCDF-*dhaA*90R	*Nde*I/*Kpn*I
			echA, hheC	pCDF-*echA-hheC*	*echA* (*Nco*I/*Hind*III), *hheC* (*Nde*I/*Kpn*I)
pETDuet-1[d]	ColE1	40	*dhaAwt*	pETDuet-*dhaA*wt	(*Nde*I/*Kpn*I)
			echA, hheC	pETDuet-*echA-hheC*	*echA* (*Nco*I/*Hind*III), *hheC* (*Nde*I/*Kpn*I)
			dhaA90R	pETDuet-*dhaA*90R	(*Nde*I/*Kpn*I)

[a]Source: Novagen. [b]CmR: chloramphenicol resistance. [c]SmR: streptomycin/spectinomycin resistance. [d]AmpR: ampicillin resistance.

$MgSO_4 \cdot 7H_2O$ and 2 mL of trace elements per 1 L and 10 mM glucose were used for toxicity tests. *Escherichia coli* DH5α (Life Technologies, USA) was used in cloning and plasmid propagation. *E. coli* BL21 (DE3) (Life Technologies, USA) was used as a heterologous host for expression of the synthetic pathway for the biodegradation of TCP. Plasmids pET21b, pACYCDuet-1, pETDuet-1, pCDFDuet-1 (Novagen, Germany) were used for subcloning and modular construction of pathway variants.

Molecular Techniques and Culture Conditions. The genes of the haloalcohol dehalogenase encoding HheC[21] and the epoxide hydrolase encoding EchA[22] from *Agrobacterium radiobacter* AD1, together with genes of the wild-type haloalkane dehalogenase from *Rhodococcus rhodochrous* NCIMB 13064 encoding DhaAwt[20] and the mutants DhaA90R[27] and DhaA31[26] were commercially synthesized (GeneArt, Germany). A tag sequence of six histidine codons was attached downstream from the gene in all cases except for *hheC*. Sequences of all genes except for *hheC* were codon-optimized for expression in *E. coli* during gene synthesis. Synthetic genes were subcloned into the *Nde*I and *Bam*HI restriction sites of pET21b. An alternative *Nco*I restriction site was introduced at the beginning of the *echA* gene to enable cloning into the first multiple cloning sites of Duet vectors. Upon introduction of the *NcoI* site, the second codon of the *echA* gene, ACT encoding threonine, was substituted for GCA encoding alanine. The constructs pET21b-*dhaA*, pET21b-*dhaA*31, pET21b-*dhaA*90R, pET21b-*hheC*, and pET21b-*echA* were used for transformation of competent cells of *E. coli* DH5α using the heat-shock method for plasmid propagation. Isolated plasmids were used for transformation of competent cells of *E. coli* BL21 (DE3) for evaluation of individual gene expression under similar conditions. Subcloning of the genes coding for the synthetic pathway into Duet plasmids is summarized in Table 2. *E. coli* BL21 (DE3) cotransformants, prepared by modular combination of recombinant Duet vectors are summarized in Table 1. All plasmid constructs were verified by sequencing (GATC, Germany).

Precultures of *E. coli* DH5α, BL21 (DE3) host cells, and cotransformants were prepared by growth on LB medium with or without antibiotics at 37 °C overnight. Final concentrations of respective antibiotics (ampicillin 100 μg/mL, chloramphenicol 34 μg/mL, streptomycin 50 μg/mL) were used in the cultures with cells containing a single plasmid. Half concentrations of two relevant antibiotics were used in precultures and cultures of cotransformants. A standard protocol was developed for the cultivation of the degraders. Precultures were used to inoculate fresh LB medium, and cultures were grown at 37 °C until the cell density reached 1 at OD_{600}. Expression of recombinant enzymes was induced by 0.2 mM isopropyl-β-D-thiogalactopyranoside (IPTG) and cultivation continued at 20 °C. Cells were harvested during the late exponential phase by centrifugation (5000*g*, 15 min, 4 °C), washed three times with sterile ice-cold SMM, M9 medium or 50 mM sodium phosphate buffer (pH 7.0), and used in further experiments.

Analytical Techniques. A gas chromatograph 6890N with a flame ionization detector (GC-FID) and mass spectrometer (GC-MS) 5975C MSD (Agilent Technologies, USA), with the capillary column ZB-FFAP 30 m × 0.25 mm × 0.25 μm (Phenomenex, USA) were used for routine analysis and quantification of TCP and its metabolites. The separation method for both GC-FID and GC-MS used an inlet temperature of 250 °C, split ratio 20:1, helium carrier gas with an initial flow of 0.6 mL/min for 1 min, followed by a flow gradient of 0.2 mL/min/min from 0.6 to 1.8 mL/min, and an oven temperature program set initially to 50 °C for 1 min, followed by a temperature gradient of 25 °C/min from 50 to 220 °C with holding for 2 min.

Determination of Toxicity of the Substrate and Intermediate Metabolites. A growth test in M9 medium containing 10 mM glucose was used to determine the toxicity of TCP and its intermediates. The growth of *E. coli* cultures was evaluated at 37 °C for 6 h using 0.5, 1, 2, 4, 5, 10, 15, and 20 mM of TCP, DCP, ECH, CPD, and GLD. To avoid the evaporation of volatile compounds, cultivation was done in 25 mL glass vials with a screw cap mininert valve (Sigma-Aldrich, USA). The concentration of TCP and intermediate compounds was monitored by GC. Samples (0.5 mL) were withdrawn and extracted with acetone (1:1), containing hexan-1-ol as an internal standard and centrifuged for 2 min at 18000*g*. The acetone extracts (2 μL) were injected directly into GC. *E. coli* cultures without the addition of the tested compounds were used as a negative control. For growth monitoring, 1 mL samples were withdrawn in 1 h intervals and measured at OD_{600}. Toxicity data were fit into polynomial equations from which the inhibitory concentration of individual compounds (IC_{20} value) was determined.

Determination of Expression Levels of the Enzymes of the TCP Pathway. The expression levels of DhaAwt, DhaA31, DhaA90R, HheC, and EchA were determined in *E. coli* BL21 (DE3) cells transformed with a pET21b vector subcloned with corresponding genes, as well as in the degraders prepared by standardized cultivation procedures. Washed cells were resuspended in 10 mL of 50 mM sodium phosphate buffer, and cell density was adjusted to 3.5 at OD_{600}. 1 U of DNaseI per 1 mL of cell suspension was added. Cells were disrupted with 5 cycles of sonication using a Hielscher UP200S (Teltow, Germany) ultrasonic processor with 0.3 s pulses and an amplitude 85%. Each cycle consisted of 5 min sonication followed by 5 min cooling at 4 °C. The cell lysate was centrifuged for 1 h at 18000*g* at 4 °C, and the resulting cell-free extract (CFE)

dx.doi.org/10.1021/sb400147n | *ACS Synth. Biol.* XXXX, XXX, XXX−XXX

was decanted. The concentration of total protein in CFEs was determined using Bradford reagent (Sigma Aldrich, USA). Samples of CFE containing 5 μg of total protein were separated by sodium dodecyl sulfate polyacrylamide gel electrophoresis (SDS-PAGE). CFE prepared from *E. coli* BL21 (DE3) cells without plasmids was used as a control. For determination of the mass ratio, the method was calibrated with standard samples containing 0.25, 0.5, 1, 1.5, and 2 μg of each enzyme DhaA, EchA and HheC in purified form. Purification of DhaA, DhaA31, DhaA90R, HheC and EchA has been described elsewhere.[29] Gels were stained with Coomassie Brilliant Blue R-250 (Fluka, Switzerland) and analyzed using a GS-800 Calibrated Imaging Densitometer (Bio-Rad, USA). The amounts of DhaAwt, DhaA90R, DhaA31, HheC and EchA in samples of CFE applied to the gel and the corresponding relative and mass ratios of the enzymes in the individual degraders were estimated from trace densities of selected bands.

Verification of Expression Levels by Activity Measurements. The expression levels of DhaAwt, DhaA31, HheC, and EchA estimated from SDS-PAGE analysis of CFE samples using deg31 and deg31-opt were verified by the measurement of individual enzyme activity in CFE. The activity of DhaA, HheC, and EchA was estimated using 10 mM TCP, 20 mM DCP, and 10 mM ECH, respectively. Substrates were dissolved in 10 mL of 50 mM Tris-SO_4 buffer (pH 8.5) at 37 °C. The reaction was initiated with the addition of CFE to a volume corresponding to 1 mg of DhaA, 1 mg of HheC or 1 mg of EchA, as was estimated from the expression levels analyzed by SDS-PAGE. CFE from *E. coli* BL21 (DE3) without plasmids was used as a negative control. Samples (0.5 mL) of the reaction mixtures were withdrawn at certain time intervals and mixed with a 0.5 mL solution of acetone in hexan-1-ol and analyzed by GC. Specific activity was calculated as a decrease in substrate concentration in μmol per min per mg of the enzyme.

Mathematical Modeling and Optimization of the TCP Pathway. The mathematical model describing the TCP pathway was constructed using kinetic equations and parameters obtained from *in vitro* enzyme kinetics with the purified enzymes and corresponding substrates (TCP, DCP, ECH, CPD, and GDL). All kinetic experiments were performed in 50 mM Tris-SO_4 buffer at pH 8.5 and 37 °C. Determination of kinetic parameters and construction of the model and its experimental verification for *in vitro* conditions is described elsewhere.[29] Initial parameters for pathway optimization were as follows: starting concentration of TCP in 10 mL reaction, 2 mM; time interval of multienzyme reaction, 300 min; total mass of enzymes in the pathway, 3 mg. Allowed combinations of Duet vectors were prepared using the following criteria: only two out of three employed Duet vector derivatives (pACYC, pCDF and pETDuet) can be combined; either one or two genes coding for enzymes from the TCP pathway can be expressed from one vector; only the *echA* gene possesses the *Nco*I restriction site for subcloning into the first multiple cloning site of Duet vectors, thus it can be expressed only from a vector with another subcloned gene and not separately. The relative ratio of enzymes in a simulation was then determined by a particular combination of plasmids carrying individual enzymes and a copy number of individual plasmids (10 for pACYCDuet-1, 20 for pCDFDuet-1, and 40 for pETDuet-1). For all allowed combinations of plasmids, dynamic simulations of the multienzyme system based on a series of Michaelis−Menten equations were performed using the Python 2.7 programming language. The differential form of equations was integrated using Euler's method with a fixed step size of 0.05 min. The toxicity effect at individual times along degradation profiles was calculated using previously obtained polynomial equations fitted to experimental toxicity data and the actual concentration of each compound at a given time. The overall toxicity effect was calculated by integration of individual effects along the profile.

Multienzyme reactions including variants of the DhaA enzyme with modified catalytic properties were modeled using the following adjustments of the previously described process. The total mass of enzymes was set to 0.1 mg, the time-interval of the multienzyme reaction was set to 24 h. A modification of the catalytic performance of DhaA was as follows: K_M was set to 1 mM, while the overall k_{cat} was varied across the range of 1 to 1000 min^{-1}. The enantioselectivity of DhaA expressed as a ratio of catalytic rate constants leading toward production of individual enantiomers of DCP was assigned for values ranging from 1 to 200. To avoid the limitation of the relative ratio of enzymes in the simulation by the employed plasmids, the mass of individual enzymes were assigned a value from 0.0 to 0.1 mg with intervals of 0.0125 mg. The ratio resulting in the highest end-point production of GLY was considered as representative of the optimized pathway.

Characterization of the Degraders in Minimal Medium with TCP. Preinduced cells of the six constructed degraders (Table 1) were washed with sterile ice cold SMM medium and resuspended in the same medium. A final concentration of 2 mM TCP was added to 15 mL of sterile SMM in 25 mL glass vials with a screw cap mininert valve (Sigma-Aldrich, USA) and incubated at 30 °C with shaking for 2 h to allow for complete dissolution. Washed cells were adjusted to a final cell density 0.1 at OD_{600}. Vials containing BL21 (DE3) cells with and without TCP were used as controls. Flasks were continuously incubated for 5 days in a shaking incubator NB-205 (N-Biotek, South Korea) at 200 rpm and 30 °C. Samples for analysis of TCP and metabolites were withdrawn at 0, 6, 24, 48, 72, 96, and 120 h. Viability of cells at the beginning and end of their incubation with TCP was tested by plating a sample of cell suspension diluted 2×10^4-times with ice-cold sterile SMM onto LB agar plates. Plates were incubated overnight at 37 °C, and grown colonies were counted using the Colony Picker CP7200 (Norgren Systems, USA).

Recovery of Degraders in LB Medium. Preinduced cells of the six constructed degraders were incubated at 37 °C with shaking in 25 mL glass vials with a screw cap mininert valve containing 10 mL of 50 mM sodium phosphate buffer (pH 7.0) with 3.5 mM TCP. The OD_{600} of cell suspensions was 3.5. BL21 (DE3) cells without plasmids were used as controls. After 5 h of incubation, cell suspension samples (10 μL) were transferred into wells of a 96-well microtiter plate containing 100 μL of LB medium. The plate was incubated at 37 °C with shaking (900 rpm) in a shaking incubator (PST-100 HL Thermo Shaker, BIOSAN). Cell growth was monitored by measuring OD_{600} at 30 min intervals using a microtiter-plate reader (Tecan, Switzerland).

Degradation of TCP in Buffer by Preinduced Resting Cells. Cell suspensions of preinduced deg31, deg31-opt and *E. coli* BL21 (DE3) without plasmids (negative control) were diluted with sterile 50 mM sodium phosphate buffer to a final OD_{600} 7. Glass vials (25 mL) with a screw cap mininert valve containing 7.5 mL of the sterile 50 mM sodium phosphate buffer of pH 7.0 and 4 mM TCP were prepared separately and incubated for 1 h at 37 °C with shaking. The reaction was initiated by mixing 7.5 mL of the cell suspension with 7.5 mL of buffer and dissolved TCP. The final concentration of TCP in 15

mL of the cell suspension was 2 mM and the final theoretical OD_{600} was 3.5. Cell suspension samples (0.5 mL) were quenched in 0.5 mL of acetone with hexan-1-ol, vortexed, and centrifuged at 18000*g* for 2 min. The concentration of metabolites in the supernatant was analyzed using GC. The presence of GLY in the cell suspension was verified using a Free Glycerol Assay Kit (BioVision, USA).

■ ASSOCIATED CONTENT

Ⓢ Supporting Information

This material is available free of charge via the Internet at http://pubs.acs.org.

■ AUTHOR INFORMATION

Corresponding Authors

*E-mail: zbynek@chemi.muni.cz.

*E-mail: jiri@chemi.muni.cz.

Author Contributions

⊥N. P. Kurumbang and P. Dvorak contributed equally.

Notes

The authors declare no competing financial interest.

■ ACKNOWLEDGMENTS

This research was funded by the SoMoPro Program (Incoming Grant SYNTBIO No. 2SGA2873 to N.P.K.) and The Grant Agency of the Czech Republic (P503/12/0572). Research leading to these results has received financial contribution from the European Community within the Seventh Framework Program (FP/2007-2013) under Grant Agreement No. 229603. The research has also been cofinanced by the South Moravian Region. Additional funding was obtained from the European Regional Development Fund (CZ.1.05/2.1.00/01.0001, CZ.1.05/1.1.00/02.0123) and the Ministry of Education of the Czech Republic (CZ.1.07/2.3.00/30.0037, CZ.1.07/2.3.00/20.0239). The work of J.B. was supported by the "Employment of the Best Young Scientists for International Cooperation Empowerment" Program (CZ1.07/2.3.00/30.0037) and cofinanced through the European Social Fund and the state budget of the Czech Republic. CERIT-SC is acknowledged for providing access to their computing facilities under the program Center CERIT scientific Cloud (CZ.1.05/3.2.00/08.0144).

■ REFERENCES

(1) Bhatt, P., Kumar, S. M., Mudliar, S., and Chakrabarti, T. (2007) Biodegradation of chlorinated compounds—a review. *Crit. Rev. Environ. Sci. Technol. 37*, 165−198.

(2) de Lorenzo, V. (2009) Recombinant bacteria for environmental release: what went wrong and what we have learnt from it. *Clin. Microbiol. Infect. 1*, 63−65.

(3) Wittich, R. M., van Dillewijn, P., and Ramos, J. L. (2010) Rational construction of bacterial strains with new/improved catabolic capabilities for the efficient breakdown of environmental pollutants, in *Handbook of Hydrocarbon and Lipid Microbiology* (Timmis, K. N., Ed.), pp 1247−1254, Springer-Verlag, Berlin.

(4) Haro, M. A., and de Lorenzo, V. (2001) Metabolic engineering of bacteria for environmental applications: construction of *Pseudomonas* strains for biodegradation of 2-chlorotoluene. *J. Biotechnol. 85*, 103−113.

(5) Cámara, B., Herrera, C., González, M., Couve, E., Hofer, B., and Seeger, M. (2004) From PCBs to highly toxic metabolites by the biphenyl pathway. *Environ. Microbiol. 6*, 842−850.

(6) Pollmann, K., Wray, V., and Pieper, D. H. (2005) Chloromethylmuconolactones as critical metabolites in the degradation of chloromethylcatechols: recalcitrance of 2-chlorotoluene. *J. Bacteriol. 187*, 2332−2340.

(7) Martínez, P., Agulló, L., Hernández, M., and Seeger, M. (2007) Chlorobenzoate inhibits growth and induces stress proteins in the PCB-degrading bacterium *Burkholderia xenovorans* LB400. *Arch. Microbiol. 188*, 289−297.

(8) de la Peña Mattozzi, M., Tehara, S. K., Hong, T., and Keasling, J. D. (2006) Mineralization of paraoxon and its use as a sole C and P source by a rationally designed catabolic pathway in *Pseudomonas putida*. *Appl. Environ. Microbiol. 72*, 6699−6706.

(9) Leonard, E., Ajikumar, P. K., Thayer, K., Xiao, W. H., Mo, J. D., Tidor, B., Stephanopoulos, G., and Prather, K. L. (2010) Combining metabolic and protein engineering of a terpenoid biosynthetic pathway for overproduction and selectivity control. *Proc. Natl. Acad. Sci. U. S. A. 107*, 13654−13659.

(10) Zhang, K., Li, H., Cho, K. M., and Liao, J. C. (2010) Expanding metabolism for total biosynthesis of the nonnatural amino acid L-homoalanine. *Proc. Natl. Acad. Sci. U. S. A. 107*, 6234−6239.

(11) Bujara, M., Schümperli, M., Pellaux, R., Heinemann, M., and Panke, S. (2011) Optimization of a blueprint for *in vitro* glycolysis by metabolic real-time analysis. *Nat. Chem. Biol. 7*, 271−277.

(12) Li, R. D., Li, Y. Y., Lu, L. Y., Ren, C., Li, Y. X., and Liu, L. (2011) An improved kinetic model for the acetone-butanol-ethanol pathway of *Clostridium acetobutylicum* and model-based perturbation analysis. BMC. *Syst. Biol. 5*, S12.

(13) Ajikumar, P. K., Xiao, W. H., Tyo, K. E, Wang, Y., Simeon, F., Leonard, E., Mucha, O., Phon, T. H., Pfeifer, B., and Stephanopoulos, G. (2010) Isoprenoid pathway optimization for Taxol precursor overproduction in *Escherichia coli*. *Science 330*, 70−74.

(14) Xu, P., Gu, Q., Wang, W., Wong, L., Bower, A. G., Collins, C. H., and Koffas, M. A. (2013) Modular optimization of multi-gene pathways for fatty acids production in *E. coli*. *Nat. Commun. 4*, 1409.

(15) Wu, J., Du, G., Zhou, J., and Chen, J. (2013) Metabolic engineering of *Escherichia coli* for (2S)-pinocembrin production from glucose by a modular metabolic strategy. *Metab. Eng. 16*, 48−55.

(16) Copley, S. D. (2009) Evolution of efficient pathways for degradation of anthropogenic chemicals. *Nat. Chem. Biol. 5*, 559−566.

(17) Samin, G., and Janssen, D. B. (2012) Transformation and biodegradation of 1,2,3-trichloropropane (TCP). *Environ. Sci. Pollut. Res. Int. 19*, 3067−3078.

(18) Kielhorn, J., Könnecker, G., Pohlenz-Michel, C., Schmidt, S., and Mangelsdorf, I. (2003) *Concise International Chemical Assessment Document 56: 1,2,3-Trichloropropane*, WHO, Geneva.

(19) Gehlhaus, M., Foster, S., Hogan, K., and Holdsworth, G. (2009) *Toxicological Review of 1,2,3-Trichloropropane*, EPA/635/R-08/010F, US EPA, Washington, D.C.

(20) Kulakova, A. N., Larkin, M. J., and Kulakov, L. A. (1997) The plasmid-located haloalkane dehalogenase gene from *Rhodococcus rhodochrous* NCIMB 13064. *Microbiology. 143*, 109−115.

(21) van Hylckama Vlieg, J. E., Tang, L., Lutje Spelberg, J. H., Smilda, T., Poelarends, G. J., Bosma, T., van Merode, A. E., Fraaije, M. W., and Janssen, D. B. (2001) Halohydrin dehalogenases are structurally and mechanistically related to short-chain dehydrogenases/reductases. *J. Bacteriol. 183*, 5058−5066.

(22) Rink, R., Fennema, M., Smids, M., Dehmel, U., and Janssen, D. B. (1997) Primary structure and catalytic mechanism of the epoxide hydrolase from *Agrobacterium radiobacter* AD1. *J. Biol. Chem. 272*, 14650−14657.

(23) Bosma, T., Kruizinga, E., de Bruin, E. J, Poelarends, G. J, and Janssen, D. B. (1999) Utilization of trihalogenated propanes by *Agrobacterium radiobacter* AD1 through heterologous expression of the haloalkane dehalogenase from *Rhodococcus* sp. strain M15-3. *Appl. Environ. Microbiol. 65*, 4575−4581.

(24) Bosma, T., Damborsky, J., Stucki, G., and Janssen, D. B. (2002) Biodegradation of 1,2,3-trichloropropane through directed evolution and heterologous expression of a haloalkane dehalogenase gene. *Appl. Environ. Microbiol. 68*, 3582−3587.

(25) Gray, K., Richardson, T., Kretz, K., Short, J., Bartnek, F., Knowles, R., Kan, L., Swanson, P., and Robertson, D. (2001) Rapid evolution of

reversible denaturation and elevated melting temperature in a microbial haloalkane dehalogenase. *Adv. Synth. Catal. 343*, 607−617.
(26) Pavlova, M., Klvana, M., Prokop, Z., Chaloupkova, R., Banas, P., Otyepka, M., Wade, R. C., Tsuda, M., Nagata, Y., and Damborsky, J. (2009) Redesigning dehalogenase access tunnels as a strategy for degrading an anthropogenic substrate. *Nat. Chem. Biol. 5*, 727−733.
(27) van Leeuwen, J. G., Wijma, H. J., Floor, R. J., van der Laan, J. M., and Janssen, D. B. (2012) Directed evolution strategies for enantiocomplementary haloalkane dehalogenases: from chemical waste to enantiopure building blocks. *ChemBioChem. 13*, 137−148.
(28) Koudelakova, T., Chaloupkova, R., Brezovsky, J., Prokop, Z., Sebestova, E., Hesseler, M., Khabiri, M., Plevaka, M., Kulik, D., Kuta Smatanova, I., Rezacova, P., Ettrich, R., Bornscheuer, U. T., and Damborsky, J. (2013) Engineering enzyme stability and resistance to an organic cosolvent by modification of residues in the access tunnel. *Angew. Chem., Int. Ed. 52*, 1959−1963.
(29) Dvorak, P., Kurumbang, N. P., Bendl, J., Brezovsky, J., Prokop, Z., and Damborsky, J. (2014). Manuscript under preparation.
(30) Novagen (2004) *Duet Vectors—User Protocol*, EMD Biosciences, Darmstadt, Germany.
(31) Nawabi, P., Bauer, S., Kyrpides, N., and Lykidis, A. (2011) Engineering *Escherichia coli* for biodiesel production utilizing a bacterial fatty acid methyltransferase. *Appl. Environ. Microbiol. 77*, 8052−8061.
(32) Zhang, C., Liu, L., Teng, L., Chen, J., Liu, J., Li, J., Du, G., and Chen, J. (2012) Metabolic engineering of *Escherichia coli* BL21 for biosynthesis of heparosan, a bioengineered heparin precursor. *Metab. Eng. 14*, 521−527.
(33) Xu, P., Vansiri, A., Bhan, N., and Koffas, M. A. (2012) ePathBrick: a synthetic biology platform for engineering metabolic pathways in *E. coli*. *ACS Synth. Biol. 1*, 256−266.
(34) Tolia, N. H., and Joshua-Tor, L. (2006) Strategies for protein expression in *Escherichia coli*. *Nat. Methods 3*, 55−64.
(35) Nikel, P. I., Pérez-Pantoja, D., and de Lorenzo, V. (2013) Why are chlorinated pollutants so difficult to degrade aerobically? Redox stress limits 1,3-dichloprop-1-ene metabolism by *Pseudomonas pavonaceae*. *Philos. Trans. R. Soc., B 368*, 20120377.
(36) Diaz Ricci, J. C., and Hernández, M. E. (2000) Plasmid effects on *Escherichia coli* metabolism. *Crit. Rev. Biotechnol. 20*, 79−108.
(37) Janssen, D. B., Pries, F., Vanderploeg, J., Kazemier, B., Terpstra, P., and Witholt, B. (1989) Cloning of 1,2-dichloroethane degradation genes of *Xanthobacter autotrophicus* GJ10 and expression and sequencing of the *dhlA* gene. *J. Bacteriol. 171*, 6791−6799.
(38) Assis, H. M. S. (1993) *Biochemical characterization of a haloalcohol dehalogenase from Arthrobacter sp. H10a*. Ph.D. Thesis, University of Kent, Kent, U.K.